JOURNAL OF MATERIALS SCIENCE 24 (1989) 1169–1176

Microanalyses of chemically etched thin film alumina–ferrite interfaces

L. M. GIGNAC*, S. H. RISBUD
University of Arizona, Department of Materials Science and Engineering, Tucson, Arizona 85721, USA

Thin films of aluminium oxide were deposited on ferrite ($Ni_xZn_{1-x}Fe_2O_4$) substrates by r.f. sputtering. The sputtered alumina films were not easily etched by hot phosphoric acid unlike readily etchable films prepared by physical deposition techniques. Microanalytical characterization of unetched films, partially etched films and interfacial regions was conducted to identify the microscopic features responsible for reluctant film etchability. The post-etched films were categorized as easily, partially and un-etchable (EE, PE and U respectively) and were examined using optical microscopy, SEM, XRD, EDS, XPS, AES, and TEM/STEM. TEM examination of cross-sections of partially etchable films revealed a non-uniform crystalline phase at the film–substrate interface. Electron diffraction data identified the phase as η-alumina although AES and EDS results suggest that the interfacial phase also contained some iron. The occurrence and orientation of the η-alumina phase was shown to depend on the orientation of the grains of the ferrite substrate.

1. Introduction

Alumina thin films are in widespread use in the microelectronics and magnetic recording industries as electrical and magnetic insulators, surface passivators, capacitor dielectrics, and diffusion barriers. A critical criterion of film quality in processing is a reasonably high chemical etch rate which allows selected areas of the film to be removed by etching and microphotolithography techniques, leaving the desired alumina pattern on the device. In general, alumina films produced at below 500° C by a host of deposition techniques (including r.f. sputtering [1–3], d.c. reactive sputtering [4, 5], evaporation [6, 7], reactive evaporation [8, 9], thermal decay of aluminium alcohoxides [10–11] and anodic oxidation [12]) have an amorphous structure. When the substrate is heated to greater than 500° C during deposition or when the as-deposited films are subsequently annealed, metastable polymorphs of alumina generically titled γ-alumina or the stable hexagonal α-alumina structures have been reported [4–6, 8–13]. Several researchers have reported that the amorphous alumina films can be etched controllably in hot H_3PO_4, HF, and buffered HF [1, 3–5, 8, 10, 11]. However, when the deposition parameters lead to crystalline (stable or metastable) alumina phase(s), the etch rate of the films decreases to almost zero [4, 5, 8, 10, 13].

Our previous work on chemically resistant alumina films deposited by r.f. sputtering utilized statistical experimental design to isolate the sputtering parameters influential in producing unetchable films on ferrite substrates. The films were non-uniform, thus experimental results pin-pointing the cause of the unetchable film structures were not obtained. While all films gave a reasonable chemical etch rate, some alumina film fragments remained on the ferrite and could not be removed after longer and harsher etching procedures. In the present study, standard etchable and unetchable alumina films were examined using a number of microanalytical characterization techniques in order to identify the microstructural aspects of the chemically resistant films and discern the cause of their formation. Optical and scanning electron microscopy (SEM), transmission electron microscopy (TEM/STEM), X-ray diffraction (XRD), X-ray photoelectron spectroscopy (XPS) and Auger electron spectroscopy (AES) were among the techniques used.

2. Experimental procedure

2.1. Film preparation and etching

Alumina, Al_2O_3, films were deposited on polycrystalline ferrite, (Ni, Zn)Fe_2O_4, substrates using a Perkin Elmer 2400 r.f. sputtering apparatus with a hot pressed alumina target. During deposition, the substrates and target were water cooled and a substrate bias between -75 and -175 V was applied. The final film thickness was approximately 0.9 μm after a 36 min deposition which produced an average film deposition rate of 24.9 nm min^{-1}.

The deposition and chemical etch rates were measured on the as-deposited alumina films. To obtain these measurements, a two-step etching procedure was used. First, a strip of black wax was applied down the centre of the top surface of the film. The film was etched in a 50% solution of H_3PO_4 heated to 50° C for 5 min. After thoroughly rinsing and drying the sample, a second strip of black wax was applied to the film surface so two-thirds of the film

*Present address: IBM Corporation, East Fishkill, New York 12533, USA.

0022–2461/89 $03.00 + .12

surface was covered with the wax. The sample was etched a second time in a 70% solution of H_3PO_4 heated to 70° C for 15 min. The wax was removed using 1-1-1-trichloroethane. A Dektak was employed to measure the film thickness and the step of the partially etched film. With knowledge of the time elapsed during deposition and etching, the alumina deposition and chemical etch rates were calculated.

Three types of films were deposited and analysed: chemically unetchable, partially etchable, and standard easily etchable films. The unetchable films were so classified, because, after thorough etching, the majority of the film remained on the ferrite. The partially etchable films were almost completely removed by the etching procedure, but a thin layer of alumina still remained on the ferrite surface. The easily etchable films were completely stripped off by the acid.

2.2. Optical and scanning electron microscopy (SEM)

After the films were etched, the samples were inspected using a Zeiss ICM-405 optical microscope and an ISI Super IIIA SEM. The area on the sample where the film was exposed to the complete etching procedure was targeted. For SEM analysis, a thin layer of carbon was evaporated on the sample surface to make the sample conducting. Energy dispersive X-ray spectra (EDS) were obtained using a PGT system III spectrometer.

2.3. X-ray diffraction (XRD)

The as-deposited etchable and unetchable thin films were examined using a General Electric XRD-5 X-ray diffractometer with monochromatic Cu$K\alpha$ radiation at a scanning rate of $2° \text{min}^{-1}$. Since the films were $\sim 0.9\ \mu$m thick, a detectable X-ray signal from the film was obtained.

2.4. Surface analytical techniques

The as-deposited and post-etched areas of the film were examined using a Vacuum Generators ESCALAB MK II X-ray photoelectron spectrometer and a Perkin Elmer PHI 600 scanning auger microprobe. The samples were sectioned and then mounted on the sample holders using DAG. A conductive coating was not deposited on the surface of the film to achieve best conditions for data collection.

2.5. Transmission electron microscopy (TEM)

The alumina–substrate interface was examined by TEM and STEM. Cross-section layered structures were prepared according to a technique described by Bravman and Sinclair [15]. Initially, two thin film surfaces were glued together using M-Bond 610* adhesive. Pressure was applied to the glued structure using a machinist clamp, and the glue was cured at 170° C for 2 h. After curing, 300 to 500 μm thick cross-section slices of the film structure were sectioned using a Buehler† Isomet slow speed diamond saw. Next, 3 mm diameter discs were cut with a Gatan‡ disc cutter, and an attempt was made to align the glued interface in the centre of the disc. This disc was ground on both sides to a thickness of $\sim 100\ \mu$m, and then both faces of the disc were polished with a diamond based media. The grinding and polishing were accomplished using the Buehler† Mini-met. A dimple, centred on the glued interface and 70 to 80 μm in depth, was ground into the disc using the Gatan‡ dimpler. Finally, the disc was ion milled using a cold stage and a low voltage gun (4 keV) in the Gatan‡ dual ion mill until a thin, electron transparent region was obtained. Fig. 1 shows optical micrographs of a prepared TEM cross-section layered structure. The cross-section samples were examined using the Philips CM 12 TEM/STEM and the JEOL 4000 TEM.

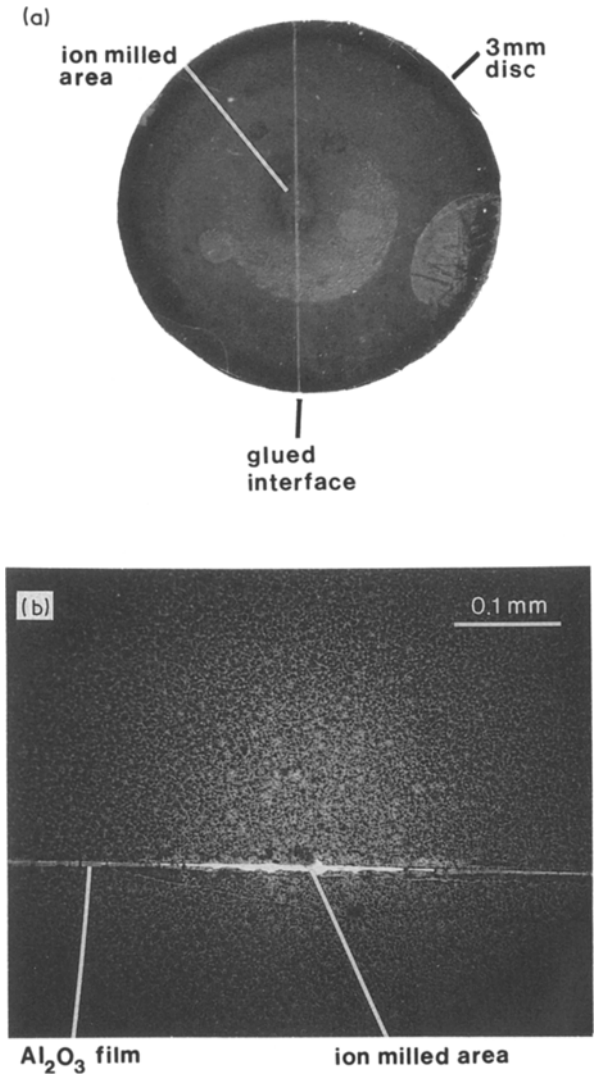

Figure 1 Optical micrographs of TEM cross-section layered structure after ion milling: (a) The glued interface, dimple, and ion milled areas of the sample are depicted. (b) Transmitted light image of the glued interface showing large ion milled area.

3. Results and discussion

Table I shows the average thicknesses and chemical etch rates of the three types of film studied. For convenience we will refer to these films as U (unetchable), PE (partially etchable) and EE (easily etchable). The

*M-Line Accessories, Measurements Group, Incorporated, Rayleigh, North Carolina, USA.
†Buehler Ltd, 41 Waukegan Road, Lake Bluff, Illinois 60044, USA.
‡Gatan Incorporated, 6678 Owens Drive, Pleasanton, California 94566, USA.

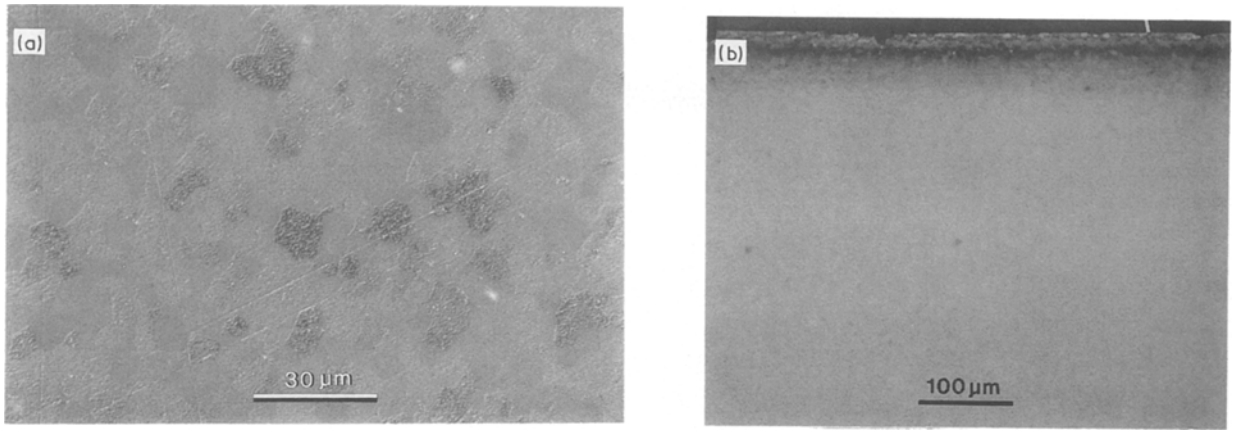

Figure 2 Optical micrograph of the top surface of a post-etched: (a) unetchable (U) film, and (b) partially etchable (PE) film.

U films were approximately as thick as the other two films; however, incomplete etching of the film produced an erroneous thickness reading using the profilometer. The U film had a very slow etch rate of $5.3\,nm\,min^{-1}$, and, after the full etching procedure, the film remained on the ferrite surface. The PE film etched at a reasonable rate, but, with extended etching periods, localized alumina structures were not removed from the ferrite surface. The EE films etched well in the acid and left no trace of the film structures.

In Fig. 2a, an optical micrograph depicts the top surface of the U film after etching in hot phosphoric acid. An alumina structure was remanent on the ferrite surface which appeared crystalline. When inspected further by SEM, three distinct regions were apparent on the ferrite surface: (i) alumina barely touched by chemical attack, (ii) alumina partially etched and (iii) alumina almost completely removed. These regions are shown in Fig. 3. The size and morphology of the region resembled the structure of the ferrite crystallites. Thus, these observations suggested that the substrate structure influences the film growth. Similar to the U films, the PE films also contained film structures after etching. As shown in Fig. 2b, a brown layer was observed on the ferrite surface after etching. At the substrate edge, the film was thicker and appeared to be more crystalline. SEM examination also indicated that the post-etched film structures were influenced by the ferrite crystallites.

Previous literature reports have concluded that chemically resistant alumina films have a crystalline (stable or metastable) structure [2, 3, 5]. In this study, the U film was believed to be crystalline alumina formed due to insufficient cooling of the substrate during deposition or by nucleation from impurities in the vacuum system. It is possible that an alumina-ferrite crystalline phase might have formed during the initial stages of deposition because a strong substrate bias was employed. X-ray diffraction analyses were used to identify the possible crystalline phases in the sample. When the U and EE films were compared, the X-ray diffraction patterns did not differ significantly as shown in Fig. 4. The X-ray peaks recorded correspond to the fcc ferrite ($Ni_xZn_{1-x}Fe_2O_4$) substrate. Since the films were relatively thick ($\sim 0.9\,\mu m$) any crystalline phase(s) in the thin film would have been detected, if present. Thus, a metastable crystalline alumina or alumina-ferrite phase is not likely on the basis of this present data. The presence of an extremely thin crystalline layer at the interface (beyond the resolution of XRD) cannot, however, be ruled out.

When analysing the samples by SEM, an energy dispersive X-ray spectrometer (EDS) was used to measure the characteristic X-ray yield in an electron irradiated as-deposited and post-etched U film. These data are presented in Figs 5a and b, respectively. The sole elements detected in both spectra were aluminium, argon, iron, nickel and zinc which comprised the elements of the substrate and the film. Significant amounts of argon were recorded in the as-deposited films due to argon entrapment during film deposition. Thus, stronger iron, nickel and zinc signals and diminished aluminium and argon signals were recorded

TABLE I Film thickness and etch rate data for the three film categories

Film type	Film thickness (nm)	Etch rate ($nm\,min^{-1}$)
U (Unetchable)	88.7	5.3
PE (Partially Etchable)	910.8	17.0
EE (Easily Etchable)	878.4	17.4

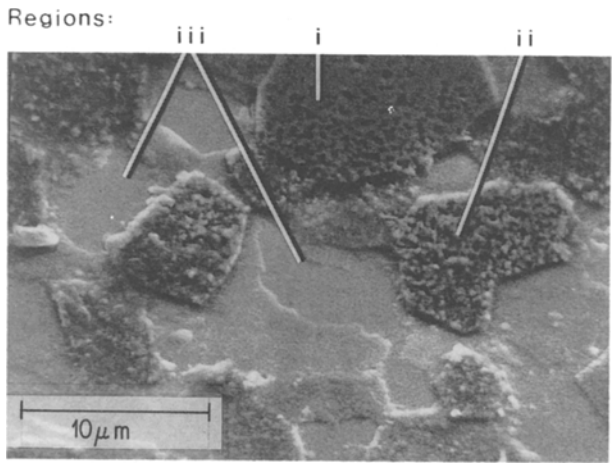

Figure 3 SEM micrograph of the U film surface after etching depicting regions where the acid: (i) barely affected, (ii) partially etched, and (iii) completely removed the film.

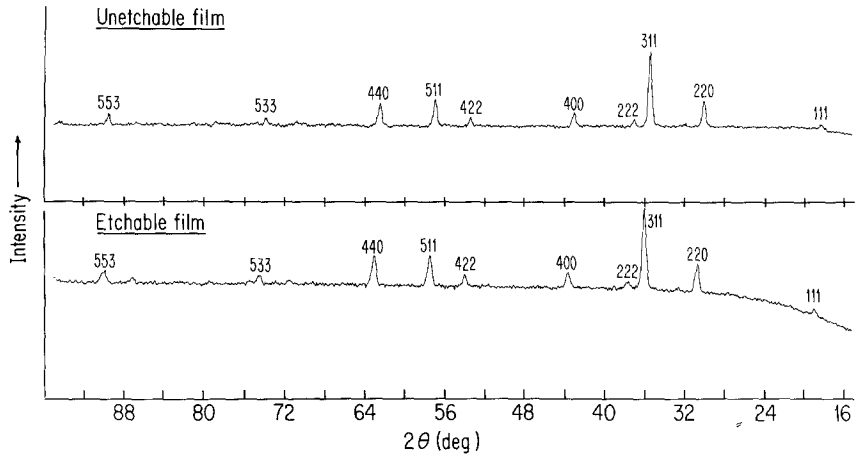

Figure 4 XRD of as-deposited etchable (EE) and unetchable (U) alumina films on ferrite substrates.

in the post-etched spectrum because less film existed on the ferrite after etching. Since no impurities were detected, the mechanism for formation of the U film probably does not involve nucleation on impurities. Since the EDS only detects elements down to sodium ($Z \geqslant 11$), the presence of low atomic number impurities is still a possibility.

Dot maps of the PE alumina film structures are shown in Fig. 6. The first micrograph (Fig. 6a) shows a backscattered electron (BSE) image of a post-etched ferrite surface with the structure of the remanent alumina film. Figs 6b and c show the aluminium and iron dot maps of this region. In the iron dot map, a high concentration of iron was recorded in the area where the alumina film structure remained. This occurred because the electron beam penetrated through the alumina film into the ferrite. Iron incorporation into the film could not be concluded from the iron dot map, but the dot maps confirmed that the film remaining on the ferrite did contain alumina.

Surface analyses were also attempted in order to detect low atomic number elements in the film and to identify the possibility of alumina–ferrite interfacial phases. X-ray photoelectron spectra (XPS) were taken from the surface of: (1) the bare ferrite, (2) the as-deposited alumina, (3) the post-etched ferrite with remanent alumina, and (4) the post-etched ferrite without alumina structures. The spectra are presented in Figs 7a to d, respectively. Since each sample was

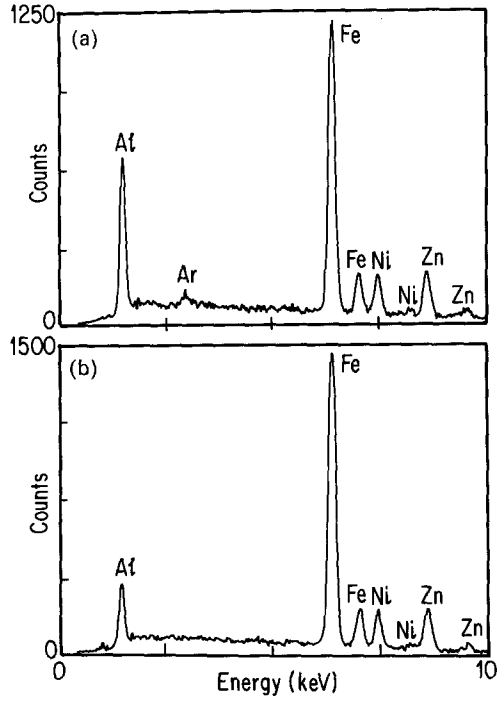

Figure 5 EDS of (U) alumina films: (a) as-deposited alumina, and (b) post etched region.

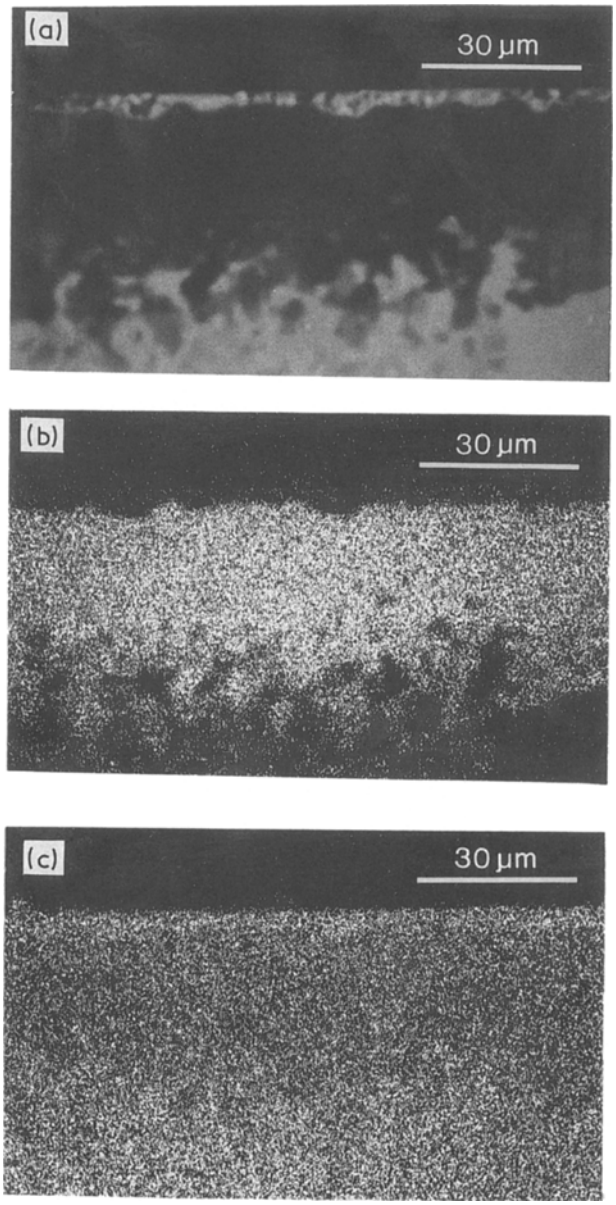

Figure 6 (a) Backscattered electron image of remanent alumina film after complete etching procedure (PE films). (b) Aluminium dot map of region in (a). (c) The dot map of region in (a).

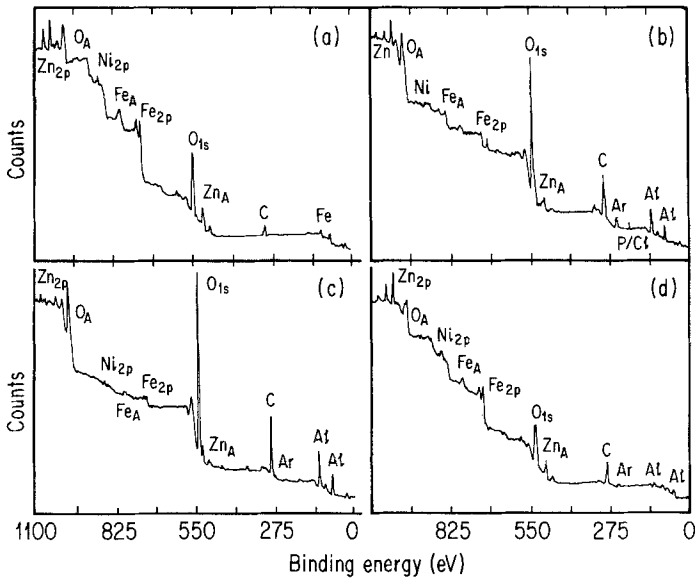

Figure 7 X-ray Photoelectron Spectra (XPS) of: (a) bare ferrite surface, (b) as-deposited EE alumina film, (c) post-etched ferrite PE film and (d) post-etched EE film.

divided into three sections (as-deposited, partially etched, and completely etched) and the X-ray beam was very broad (~ 1 cm diameter), the XPS analyses might have incorporated data from overlapping regions. In Fig. 7b, the as-deposited alumina was inspected and nickel, zinc and iron peaks should not have been detected. If the beam overlapped the etched film portion of the sample, the metal peaks for these elements would have been expected. In the post etched sample with remanent alumina structures (Fig. 7c), considerable amounts of oxygen, carbon and chlorine were observed, and these impurities were caused from surface contamination. Otherwise, the most prominent difference between the post-etched sample with remanent alumina and the as-deposited alumina was the small amount of argon in the post-etched

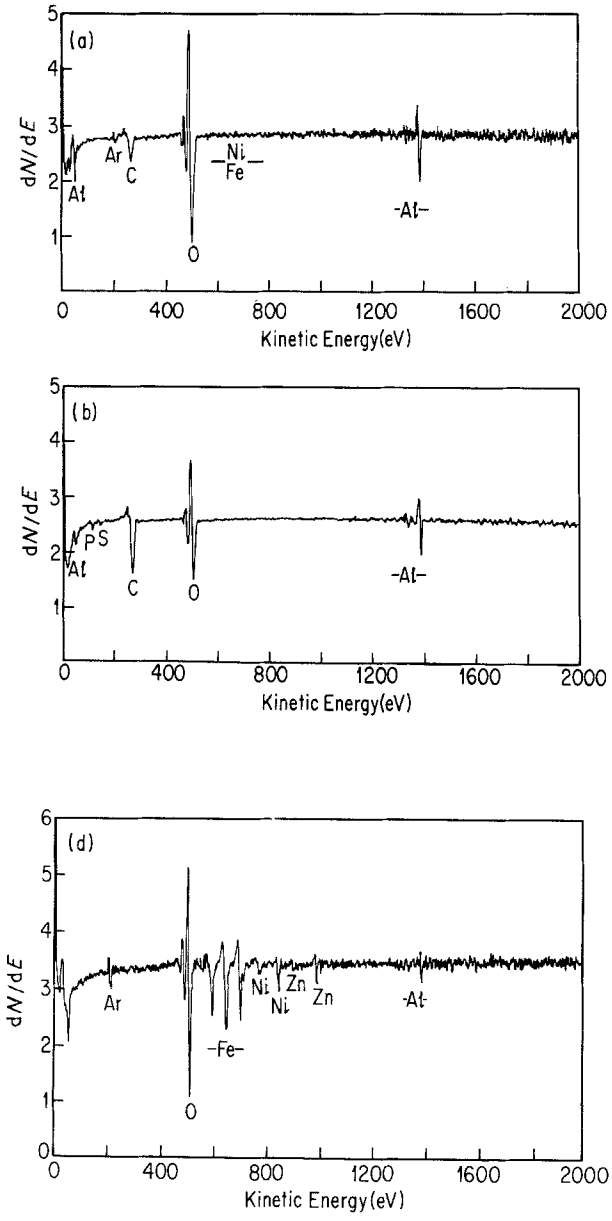

Figure 8 Auger spectra of partially etchable film. (a) survey of as-deposited film, (b) initial survey of post-etched (PES) surface, (c) survey of PES after 10 min of sputtering, (d) survey of PES after 13.5 min of sputtering, (e) profile of oxygen, aluminium, nickel, iron and zinc relative concentrations obtained during 20 min sputtering.

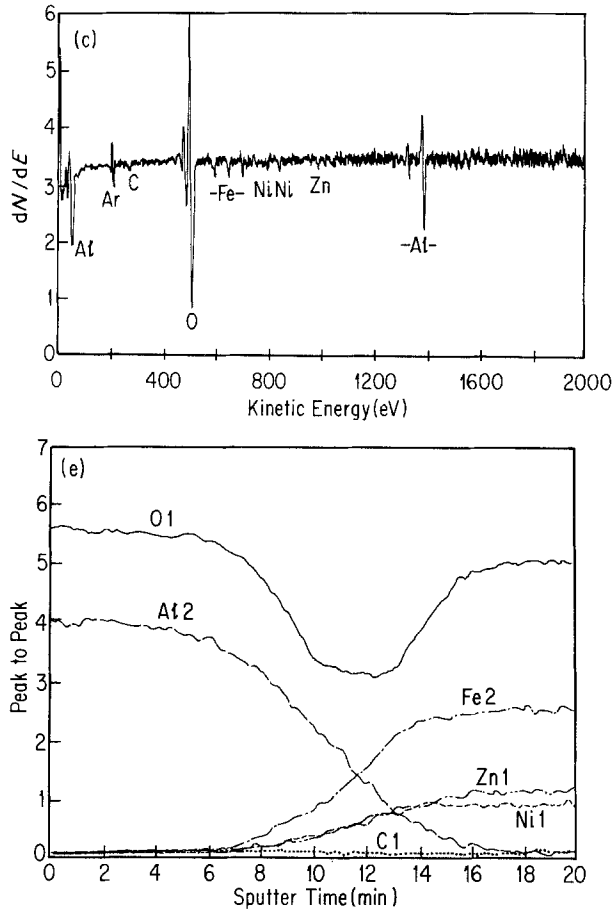

remanent alumina. The post-etched sample without remanent alumina (Fig. 7d) had a virtually identical spectra to the bare ferrite (Fig. 7a). Therefore, ferrite–alumina phase formation in the unetchable film could not be concluded from XPS data, and auger electron spectroscopy was used to obtain surface spectra with improved lateral resolution.

Auger electron spectroscopy (AES) was performed on the PE film sample, and the data is shown in Figs 8a to e. Figs 8a and b show the initial surveys of the as-deposited film surface and post-etched film surface respectively. Both surveys showed sizeable amounts of carbon, aluminum and oxygen. These elements were expected from surface contamination and the Al_2O_3 film content. Another feature shared by the two surveys was the lack of metal peaks which suggested that zinc, nickel and iron were not incorporated into the surface of the as-grown film nor the post-etched remanent structure. Since argon was observed in the as-deposited film, and not in the post-etched film structure, a lack of argon in the remanent structure was inferred. However, the detection efficiency for argon by AES is low, and the argon deficiency in the post-etched sample may be an aberration. Also, the post-etched sample contained small peaks for sulphur and phosphorus. The source of the sulphur probably was a slight amount of surface contamination, while the phosphorus peak could have been product of incomplete etching of the film by H_3PO_4. Past studies have shown that, when etching crystalline alumina with H_3PO_4, various aluminium-phosphate residues remain on the surface depending on the concentrations of the reactants and the pH of the solution [16].

Analysis of the post-etched structure was also conducted as an argon ion beam sputtered away the surface atoms at a rate of $\sim 3 \pm 1\,\text{nm}\,\text{min}^{-1}$. Surveys taken at 10 min and 13.5 min of sputtering times are shown in Figs 8c and d. A profile of the relative concentrations of oxygen, aluminium, iron, nickel and zinc measured throughout the 20 min of sputtering is given in Fig. 8e. In the 10 min survey, the occurrence of small nickel, iron and zinc peaks were initially noted, while, in the 13 min survey, these peaks intensified. From the concentration profile, the interface between the film and the ferrite can be estimated to lie at a distance corresponding to between 8 and 14 min of sputtering (~ 42 nm in thickness). This interfacial region was extremely wide considering the alumina was deposited on a cooled substrate. The result of the data strongly suggested that nickel, zinc and iron atoms were incorporated into the film near the interface up to a thickness of ~ 50 nm.

Cross-sectional TEM samples were prepared for the as-deposited partially etchable films, and TEM micrographs of this sample are presented in Figs 9 and 11. In Fig. 9, the alumina film (light in contrast) and the ferrite substrate (dark in contrast) are shown in cross-section. At the ferrite–alumina interface, a polycrystalline, non-uniform phase is visible. The phase varies in thickness from 20 to 50 nm. A diffraction pattern of the interfacial region is shown in Figs 9b and c. The pattern contains faint rings, and two sets of

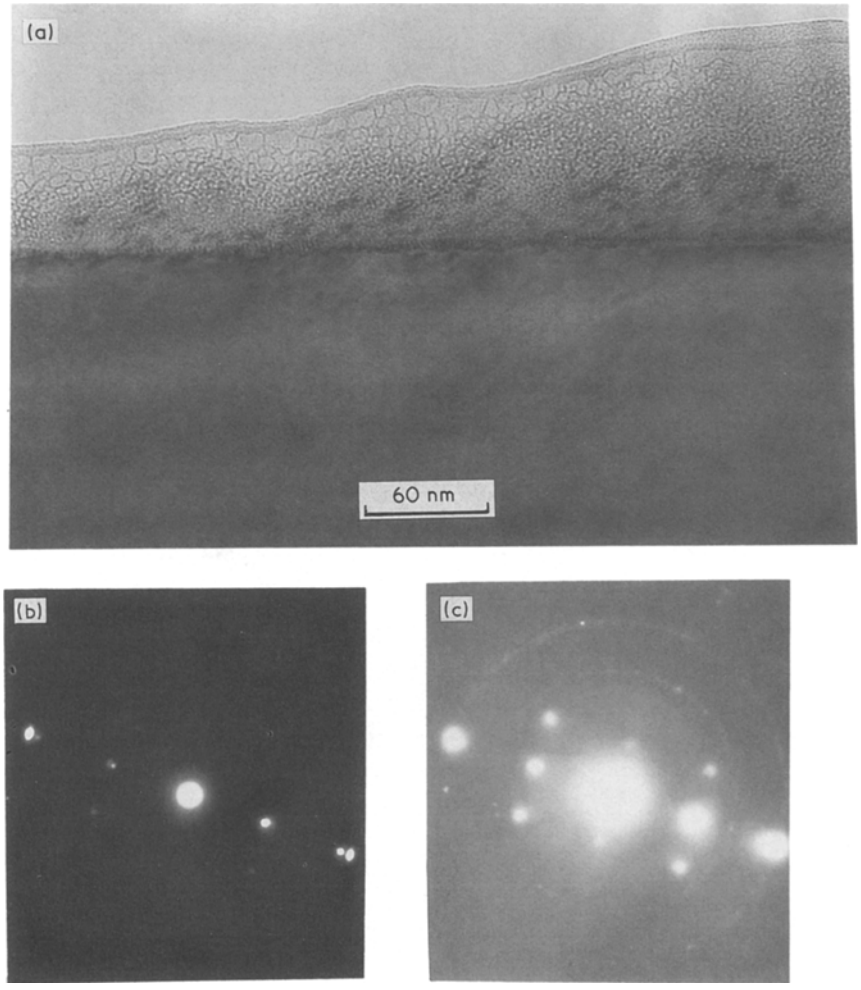

Figure 9 (a) TEM micrograph of the PE film. (b) SAD pattern of the interface showing the two sets of diffraction spots. (c) As (b) but shorter exposure when printing the negative. The faint rings related to the second set of diffraction spots are apparent.

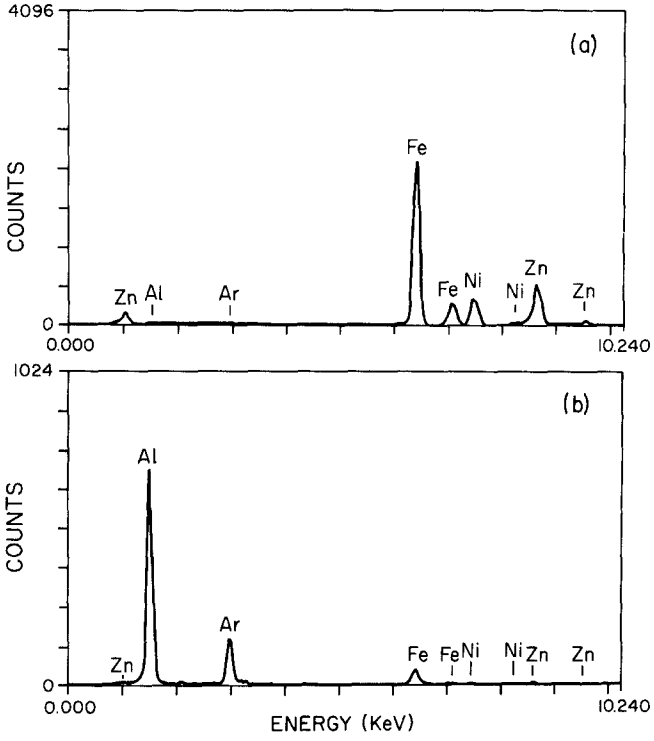

Figure 10 Energy dispersive spectra of the PE film sample (a) spectra taken in the ferrite, and (b) spectra taken in the film near the interface.

diffraction spots. The first set of dots represents a fcc structure with a lattice parameter of 0.843 ± 0.005 nm, while the faint rings along with the second set of spots depict an fcc structure with $a = 0.789 \pm 0.004$ nm. From the JCPDS powder diffraction card file, ferrite and η-alumina have fcc structures with lattice parameters of 0.8399 nm and 0.794 nm, respectively. These data suggest that the polycrystalline interfacial phase is η-alumina, a metastable polymorph of aluminium oxide. As the second set of spots were related to the rings, the interfacial phase is composed of crystallites preferentially oriented in the direction of the substrate crystal.

Two EDS spectra were recorded in the STEM and are shown in Fig. 10. Both spectra were obtained near the substrate–film interface, however, one was centred in the ferrite and the second was focused in the film containing the interfacial phase. The ferrite spectra measured only iron, zinc and nickel atoms, and the film spectra detected aluminium and argon along with a small quantity of iron. Though the electron diffraction data suggest that the interfacial phase was η-alumina, the EDS and AES results raise the possibility of a mixed phase containing alumina with ferrite.

Finally, the TEM images were helpful in explaining non-uniformity of the films. As shown in Fig. 11, a grain boundary in the ferrite travelled to the film–substrate interface. Above one side of the grain boundary, the η-alumina phase was noticed, while on top of the adjacent substrate grain, no interfacial phase was visible. The substrate crystal structure not only influenced the orientation of the η-alumina phase, but also controlled the possibility of its growth.

4. Conclusions

A variety of microanalytical characterization techniques leads to the conclusion that the non-uniform etching of sputtered aluminium oxide thin films is caused by the formation of a fine crystalline phase at the film–substrate interface. Electron diffraction patterns identified this phase as η-alumina, while AES and EDS data may also lead to the conclusion that the interfacial phase has iron dissolved from the ferrite substrate. Optical microscopy, SEM and TEM studies suggest that the crystal orientation and growth capability of the interfacial phase depends on the orientation of the ferrite grains of the polycrystalline

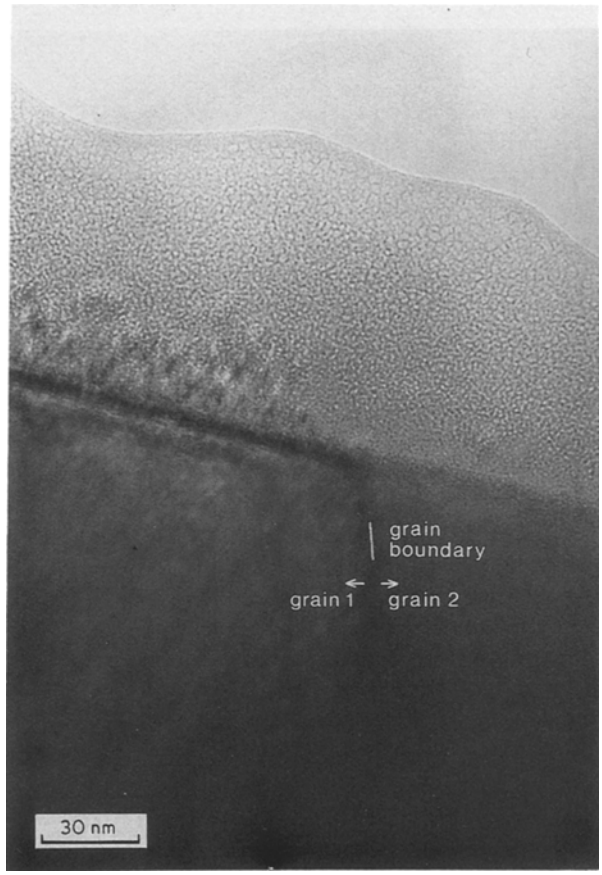

Figure 11 TEM micrograph of the PE film. The interfacial phase is discontinuous over the ferrite substrate.

substrate. Since one possible source of the undesirable etching quality of the films has been identified, our continuing research is focusing on tracing the origins of interface phase formation to the sputter processing parameters.

Acknowledgements

This work is based on L. M. Gignac's PhD thesis. We would like to acknowledge the support of the IBM Corporation and helpful discussions with S. A. Schubert and K. E. Sickafus of IBM-GPD in Tucson, Arizona.

References

1. C. A. T. SALAMA, *J. Electrochem. Soc.* **117** (1970) 913–917.
2. I. H. PRATT, *Solid State Tech.* **12** (1969) 49–57.
3. R. A. GARDNER, P. J. PETERSON and T. N. KENNEDY, *J. Vac. Sci. Tech.* **14** (1977) 1139–45.
4. R. G. FRIESER, *J. Electrochem. Soc.* **113** (1966) 357–60.
5. T. TANAKA and S. IWAUCHI, *Jpn J. Appl. Phys.* **7** (1968) 1420.
6. A. L. DRAGOO and J. J. DIAMOND, *J. Amer. Ceram. Soc.* **50** (1967) 568–574.
7. M. G. MIER and E. A. BUVINGER, *J. Vac. Sci. Tech.* **6** (1969) 727–30.
8. E. FERRIEU and B. PRUNIAX, *J. Electrochem. Soc: Solid State Sci.* **116** (1969) 1008–1013.
9. R. F. BUNSHAH and R. J. SCHRAMM, *Thin Solid Films* **40** (1977) 211–216.
10. J. A. ABOAF, *J. Electrochem. Soc: Solid State Sci.* **114** (1967) 948–952.
11. M. T. DUFFY and A. G. REVESZ, *ibid.* **117** (1970) 372–377.
12. D. J. BARBER, *J. Electrochem. Soc.* **112** (1965) 1143–1145.
13. K. IIDA and T. TSUJIDE, *Jpn J. Appl. Phys.* **11** (1972) 840–849.
14. L. M. GIGNAC, S. H. RISBUD, J. V. PRIDANS and S. A. SCHUBERT, "Statistical Experimental Design used to Evaluate Alumina Thin Films", IBM, Tucson, Internal Progress Report, Contract No. S-509805, January 1987, unpublished.
15. J. C. BRAVMAN and R. C. SINCLAIR, *J. Electron. Microsc. Tech.* **1** (1984) 53–61.
16. F. J. GONZALEZ and J. W. HALLORAN, *Bull. Amer. Ceram. Soc.* **59** (1980) 727–731.

Received 29 February
and accepted 18 July 1988